Simultaneous detection of copper, lead and mercury in river water with in-situ pH control using electrochemical stripping techniques

Bernardo Patella [a,b], Benjamin O'Sullivan[a], Robert Daly[a], Pierre Lovera [a,] Rosalinda Inguanta[b], Alan O'Riordan[a]

a Nanotechnology Group, Tyndall National Institute, University College Cork, Cork T12R5CP, Ireland

b Università di Palermo, Laboratorio di Chimica Fisica Applicata, Dipartimento dell'Innovazione Industriale e Digitale, Ingegneria, Chimica Gestionale Informatica Meccanica, Università di Palermo, Viale delle Scienze - 90128 Palermo (Italy)

KEYWORDS: Sensors, Gold, Microbands, local pH, heavy metal, in situ, real time, lead, mercury, contamination

ABSTRACT: An electrochemical sensor for the detection of lead, mercury and copper in neutral solutions is described. The electrode is made of two distinct parallel gold interdigitated microband electrodes that can be polarized separately. Biasing one electrode "protonator" sufficiently positive to begin water electrolysis, results in the production of H^+ ions which consequently drops the pH in the locality around the other second interdigitated "sensing" electrode. This decrease in pH permits the electodeposition (and consequent stripping) of metals at the sensing electrode without the need to acidify the whole test solution. In this work, the local pH can be adjusted from 1 to 7 in a stable and reproducible way by tailoring the applied potential to the protonator electrode. Using this approach, linear ranges for lead 10-100 ppb, copper 5-100 ppb and mercury 1-75 ppb, respectively were demonstrated which exhibit extremely high sensitivity. This technique allowed detection of these metals in a complex water matrix (river water) without sample pretreatment, with excellent results. The electrode reproducibility is high (RSD < 10%) and the metals can be co-detected when present all together. This is the first demonstration of the in-situ pH control for heavy metal detection using solid state sensors and will unable real time and in situ analysis of heavy metals by unskilled personnel in remote settings.

Introduction

Water is a precious resource, being key to various economic activities such as transport, agriculture, manufacturing, tourism/entertainment and, of course, a major health component through consumption. Unfortunately, multiple threats to water quality are associated with a variety of fields of use: pollution from pesticides used in agriculture, polycyclic aromatic hydrocarbons (PAHs) from incomplete combustion processes, heavy metals from manufacturing and antibiotics from human consumption, to name but a few. The European Union adopted the Water Framework Directive (WFD) in 2000 [1] set clear objectives to tackle the wide variety of contamination in order for a "good status" to be obtained for all ground and surface waters in the EU. In Europe as a whole, the EU commission reported in 2018 that around 40 % of surface water met the good status criteria [2]. While Member States have made marked efforts to improve water quality, new contaminants not currently monitored are emerging. One of the challenges faced by the Member States regarding the monitoring of priority substances is the lack of robust, reliable and cost-efficient methods of detection for a

number of these contaminants. However, at the same time, the commission recommends to "improve and expand monitoring and assessment tools to ensure a statistically robust and comprehensive picture of the status of the aquatic environment for the purpose of further planning" [1]. Outside of Europe, the United Nations Sustainable Development Goals are a call for action by all countries to promote prosperity while protecting the environment [3]. Real-time analysis for Pollution Prevention; typically employing point-of-use sensor systems [4-6]. These provide an immediate analytical response to stakeholders allowing them, in some cases, to undertake rapid interventions on the spot. Ironically, a majority of point-of-use chemical test kits for pollutant analysis, require the addition of chemical reagents that, in themselves, need specialized waste disposal. For example, chemical oxygen demand products contain sulphuric acid and mercury (II) sulphate while heavy metal analysis requires samples to be acidified with nitric acid to aid of metal digestion [7-8]. Furthermore, from an analytical perspective, addition of chemical reagents brings along extra challenges, e.g., they are a potential source for interferants and contaminants in trace analysis, have associated chemical hazard handling and management issues, increase the number of steps and thereby cost, and increase the potential for mistakes and handling errors to occur. It is very obvious therefore, that eliminating the need for addition of chemical reagents in point-of-use chemical analyses would have many wide ranging benefits.

To address these challenges, we are exploring the application of electrochemical processes couple with electrode design to tailor the chemistry of a solution both temporally and spatially at a sensor surface. Using this approach, it should be possible, in some cases, to eliminate the requirement for any reagent addition using such an approach. Heavy metals are a major source of pollution and toxicity in water. For example, the world's health organization recognizes mercury as one of the ten most dangerous chemical for human health. Mercury pollution arises mostly from several industrial sources and a weekly intake above 4µg/kg can lead to degradation of DNA and the central nervous system [9-10]. The American Environment Protection Agency (US-EPA) stating that more than 11.5tons per year of mercury waste are produced from gold mining alone [11]. Similarly, lead is readily absorbed by the body, and once ingested, has been linked to cancer, osteoporosis, psychosis, damage to kidneys and the nervous system. [12] While lead, in the form of tetraethyl lead, has been removed from gasoline, it can still be readily found in water and wastewater transported through lead pipes and also in lead-acid batteries. Finally, copper toxicity is typically manifested by the development of liver cirrhosis with episodes of hemolysis and damage to renal tubules, the brain, and other organs [13]. Consequently, the US EPA have set the maximum concentration of these metals in drinking water as 2 ppb for mercury, 15ppb for lead and 1.2ppm for copper, respectively [14] while the European Union water framework directive values of 14 ppb for lead and 0.07 ppb for mercury, respectively. [15]

The most commonly used approaches for detection of heavy metals are Atomic Absorption/Emission Spectroscopies, and inductively coupled plasma-mass spectrometry, [16-17] which provide impressive sensitivity, selectivity, limit of detection (LOD), reproducibility and accuracy. However, these approaches are extremely expensive (equipment and operational costs), are lab based, require highly skilled personnel, and are not suitable for in situ and real time analysis [9]. By contrast, electrochemical methods, including Cyclic Voltammetry (CV), Differential Pulse Voltammetry (DPV), Square Wave Anodic Stripping Volt-ammetry (SWASV), have recently emerged as effective candidates for rapid analysis of trace heavy metals [18-20]. These approaches offer performances on a par with classical analytical methods, but have advantages in that they are: easily miniaturized and thus portable, have low power consumption, are user friendly and enable real-time analysis all at significantly lower cost [18-22].

Recently, it has been shown by Read et al. that using a ring disk electrode configuration, comprising two concentric rings with a gap of 440 µm, it is possible to tailor the local pH and detect mercury at a concentration of 200 ppm in deionized water without acidifying the solution [23]. In this paper, we build on this work and present a silicon chip-based platform where each sensor comprises of two gold interdigitated electrodes, IDE, microband arrays (separated by a gap of 2 µm) that permits detection of multiple heavy metals in water. A proton diffusion simulation study is first undertaken to inform the design of interdigitated electrode sensors. This approach enables pH control, by using one electrode as a protons generator (protonator) and the other electrode as the sensing electrode. In our approach, we first demonstrate heavy metal detection using traditional chemically (acidified) pH control to optimize the experimental parameters. We then demonstrate reagent free detection by using one of the IDEs to generate protons according to reaction 1.

$$2H_2O \rightarrow O_2 + 4H^+ + 4e^- \quad (1)$$

The protons produced at a protonator electrode results in a decrease in the pH of the water solution in the vicinity of the other IDE enabling detection of Hg, Pb and Cu detection with measured LODs of 1 ppb, 100 ppb and 1 ppb, respectively. Consequently, using this method, we show it is now possible to easily detect a range of heavy metals, including mercury, lead and copper in unfiltered river water without the need for additional reagents.

Experimental

Fabrication and characterization of gold microbands

On-chip interdigitated gold microband electrode arrays were fabricated using standard microelectronics fabrication techniques on Si/SiO2 substrates as described in de-tail previously [24]. In brief, interdigitated gold micro-bands, (1 µm wide, 2 µm gaps, 45 µm long) were patterned in resist by photolithography metal evaporation (Ti/Au 5/50 nm) followed by lift-off. A second photolithography, metal evaporation (Ti/Au 10/90), and lift-off step was employed to overlay electrical interconnection tracks including peripheral probe pads and on-chip counter electrodes. Finally, a silicon nitride passivation layer (500 nm thick) was deposited to passivate the entire chip and windows selectively opened with a dry etch to allow exclusive contact between the gold microbands and the gold counter electrodes with the solution of interest. Openings were also patterned above peripheral contact pads to permit electrical connection. Chip contained 6 sensors, comprising of two interdigitated gold microbands arrays, each of which could be independently electrically polarized. A sensing electrode contains 13 microbands while A protonator electrode has 14 microbands.

Materials, Standards, Electrochemical measurements

Nitric acid (35%), Sodium Chloride, Ferrocyanide, Phosphate Buffer tablet (PBS), lead stock solution for ICP analysis (1000 ppm), mercury chloride and copper chloride powder were purchased from Sigma Aldrich (Dublin) and used as received. All solutions were prepared with DI water (resistivity of 18MΩ cm-1). All electrochemical measurements were carried out using a CHI920 bi-potentiostat in a four electrodes setup comprising two working electrodes, an on-chip counter electrode and an Ag/AgCl external reference electrode, at room temperature. Prior to the stripping experiments, the chips were washed with isopropanol and deionised water to remove any residual contaminants from the electrode surface. To characterize the electrochemical behavior of an electrode, CVs (scan rate 100mV.s-1) were carried out in a

solution containing 1 mM of ferrocyanide in 10 mM of PBS pH 7.4. Heavy metal solutions were prepared by dilutions of the stock solutions in a solution of 10 mM NaCl in DI. For chemically modified pH experiments, nitric acid was added to adjust pH and different deposition times, pH's and potentials were assessed to optimize experimental conditions. Calibration curves were obtained by undertaking measurements in triplicates using as-prepared standards and an LOD calculated using equation 2:

$$LOD=(3.3\ SD)/S \quad (2)$$

Where SD is the standard deviation of the blank and S the sensitivity of the electrode, defined as the slope of the calibration line [24].

Proton simulations towards pH control

A diffusion model was designed to model proton generation and diffusion arising at an interdigitated array and simulated using finite element analysis (COMSOL Mul-tiphysics 5.3) consistent with the galvanostatic model shown by Read et al.[25]. The geometry of the model consisted of a 5 mm square box as the experimental domain, and two sets of interdigitated (1 µm wide microband electrodes, 14 protonator microbands and 13 sensing micro-bands), separated by 2 µm. A flux of protons was applied at the surface of one IDE (protonator) by applying a fixed anodic current. The flux was assumed to be proportional to a galvanostatic current applied at the electrodes. The initial solution pH was set to pH 7. The proton diffusion coefficient used for the simulation was 9.31 x 10-5 cm 2 s -1 [26]. Diffusion of protons from the protonator was mod-eled in accordance to Fick's second law.

River water analysis

River water samples, River Lee, Cork, Ireland, were collected in three different days and three different spots and allowed to stand to allow particulates to settle. A standard addition method was carried out for the quantification of copper, lead and mercury using the supernatant samples. A minimum of five repetitive scans were carried out for each sample.

Results and discussion

Silicon chip electrochemical characterization

An optical micrograph of the chip is shown in Figure 1(a). Each chip contained 6 different gold based interdigitated electrodes with a gap of 2µm and 1 µm wide, Figure 1(b).

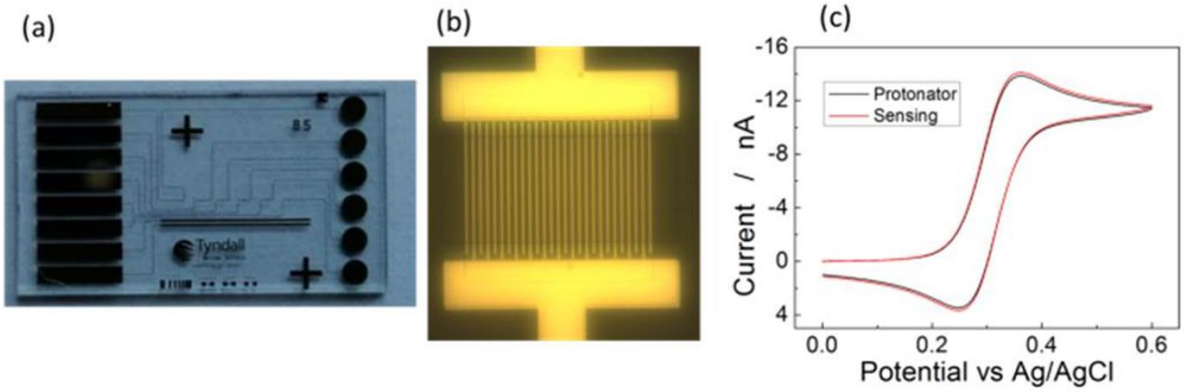

Figure 1 (a) IDEs chip containing (b) interdigitated gold microbands. (c) CV recorded using protonator and sensing electrodes in 10mM ferrocynide pH 7.4

In addition to protonator and sensing electrodes, the chip contains a silver pseudo reference electrode and a gold counter electrode. Each electrode (protonators, sensing, reference and counter) is connected to a potentiostat through a gold pattern that terminates with circular and rectangular pin outs for the external contacts. The images clearly shows the absence of any electrical shorts between sensing and protonator electrodes demonstrating that the lit-off process is highly reproducible. In order to characterize the two electrodes, CVs in presence of 1 mM ferrocyne were carried out, Figure. 1c. The two voltammograms exhibit almost the same peak current of about 14 nA. Furthermore, the peak shape suggest that the micro-band are not diffusional independent, as expected. [27-28].

To optimize sensor performance, various parameters such as pH, deposition time (td), and deposition potential (Vd) were investigated for each metal. The metal concentration was fixed at 100 ppb for copper and lead while 10 ppb was selected for mercury, due to its higher toxicity. It was observed that varying the pH significantly affected the process, in accordance with literature reports [29]. Stripping peak currents increased in more acidic media and reached a maximum at pH 3.5 for mercury and lead, and pH 2 for copper, following 3 minutes of deposition at -0.4V (see Figure S1a). This may be attributed to an increase in the metal solubility in more acidic media. With decreeing pH, the peak current were observed to reach a maximum and the decrease due to the occurrence of the hydrogen evolution reaction. For each metal, the influence of the deposition potential was investigated in the range of -0.8V to 0 V (using the optimized pH). Moving from anodic to more cathodic potentials, the output signal increased to a maximum at -0.4V for copper and lead, and -0.5V for mercury, see FigureS1b. The peak currents started to decrease at more cathodic potentials, again due to the onset of hydrogen evolution [30]. In Figure S1c is shown the effect of the deposition time, in a range from 1 to 300 s, at the optimal pH and Vd, and the current peak increased with time because the coverage on the electrode surface increased [31]. However, the current peaks reach a plateau, probably due to surface saturation [32], after 180, 180 and 120 sec for copper, lead and mercury, respectively. Table S1 summarizes the optimal parameters for each metal. During simultaneous detection of different metals, when only one deposition time can be used, detection was undertaken following 180 s of deposition.

SWASV analysis of Lead, Copper and Mercury

In order to ensure the absence of peaks in the blank solution, SWASV was carried out in a solution containing 10 mM NaCl and nitric acid only. As can be seen in Figure S2, a broad peak at -0.4V vs. Ag/AgCl, was observed, possibly due to dissolved oxygen reduction [33-35]. Figure 2a shows a CV obtained in the presence of 10 ppm of lead. Three different anodic peaks at -0.17V, -0.3V, and -0.6V vs. Ag/AgCl were observed, and attributed to under potential deposition peaks (0.17V and -0.3V) and bulk deposition (-0.6V). This behavior is consistent with previous publications on lead stripping at gold electrodes and corresponds to the formation, and consequent stripping, of a monolayer of lead at potentials more positive than the Nernst one [36-39]. Indeed, at low concentrations, only the peak at -0.17V vs. Ag/AgCl was observed, confirming that it is related to an under potential deposition. Square wave voltammograms acquired at increasing metal (Pb) concentrations following standard addition are shown in Figures 2b. A corresponding calibration line exhibiting a high R^2 value, 0.996, is shown in Figures 2b: inset. For all the metals, the sensitivity is higher at low concentration and starts to decrease with increasing metal concentration, in agreement with the literature [19]. In the case of lead (Fig2b), at low concentration, it can be seen that the onset of the oxygen peak overlaps with the lead stripping peak, leading to a decrease in the sensitivity of the

electrode. This is confirmed in Figure S3 where a solution with 10 ppb of lead has been degassed for 30 min with N_2. After 300s of deposition in a degassed solution, the current peak is almost trebled, increasing from 80 pA to 210 pA. Figure 2 (c and d) show the corresponding experiment for Cu and Hg, respectively. In our experiments, without degassing, the LOD achieved were 1.3, 0.9 and 2.1 ppb for lead, copper and mercury respectively (see TableS2).

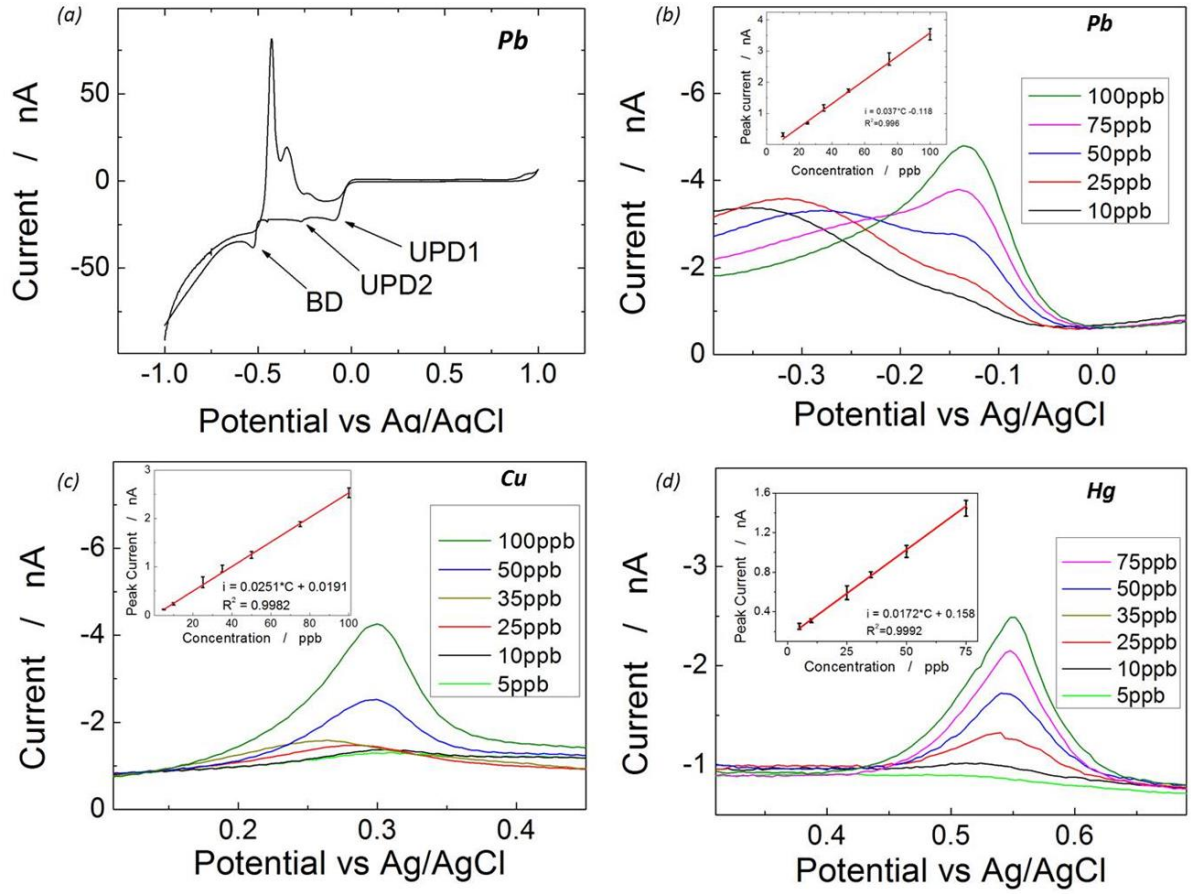

Figure 2 (a) CV in 10 ppm of lead, effect of increasing concentration of (b) lead, (c) copper and (d) mercury. Insets of figures b, c and d shows the corresponding calibration lines (insets)

In this context, it is important to highlight that for lead and copper the LOD is lower than the concentration limit settled by both US and EU EPA, while for mercury, an improvement is necessary. For this reason, the concentration range from 1 to 5 ppb has been investigated by increasing the deposition time up to 6 minutes. Figure S4 shows the stripping step from 1 to 5 ppb of mercury evidencing that it is possible to reach lower concentration by increasing the deposition time. These LODs fits with the legislation of US-EPA but not with the EU one. However, considering the deep effect of the deposition time it should be easy to decrease the LOD just increasing the deposition time or by using a microfluidic system that increase the turbulence of the system. Table 1 summarizes all the features of the electrode in terms of linear range, sensitivity and LOD. According to the above results, it can be concluded that Au based MAE can be efficiently used to detect heavy metals. Their performance is excellent in comparison with other Au based sensing electrodes with similar morphologies or other kind of nanostructured based electrochemical sensors as shown in Table 1. In order to back compare the sensitivity of the sensor, developed herein, with the literature, the sensitivities (as measured by the slope) shown in Fig2 were divided by the active area of the sensing electrode and

expressed as current density. Sensitivity is a key requirement in sensor devices as higher sensitivity enables better discrimination of smaller changes in signal readout.

Table 1 Features of different gold based electrodes for heavy metals detection

CPE = Carbon Paste Electrode; GO = Graphene Oxide; NWs = Nanowires; GCE = Glassy Carbon Electrode; TA = Terephthalic acid; rGO = reduced graphene oxide; CMS = Carbon Microspheres; SNACs = Spherical Nanoparticle Activated Carbon

	Heavy Metals	***Linear Range ppb***	***LOD ppb***	***Sensitivity μA ppb^{-1} cm^{-2}***	***Ref***
Fluorinated GO	*Cu* *Pb* *Hg*	*62.5-375* *62.1-1035* *200-1200*	*NS* *2.07* *NS*	*0.866* *0.402* *0.291*	40
Bi- exfoliated graphite	*Pb* *Hg*	*1-250* *1-250*	*0.053* *0.081*	*57.3* *70.9*	41
MnO_2 NWs-Ni foam	*Cu*	*6.25-1125*	*10.8*	*8.42*	42
Co_3O_4 nanosheets	*Pb*	*1-100*	*0.52*	*0.163*	43
NiO-GCE	*Pb*	*41.4-207*	*16.56*	*0.92*	44
TA capped Fe_2O_3 NPs - GCE	*Pb* *Hg*	*82.8-227* *80-220*	*8.28* *60*	*0.339* *0.218*	45
Chromium Oxide NPs - CPE	*Pb* *Cu*	*10-800* *10-800*	*3* *3*	*0.0566* *0.1104*	46
CPE-EDTA	*Hg*	*4.6-19*	*3.3*	*0.0041*	47
Carboimidazole grafted rGO	*Hg* *Pb*	*0.12-200* *1-240*	*0.04* *0.62*	*5.68* *0.532*	53
Paper based microfluidic carbon based sensor	*Pb*	*5-100*	*1.8*	*0.404*	54
NH_2-CMS	*Pb*	*103.5-248.4*	*11.17*	*0.688*	55

	Cu *Hg*	*31.25-75* *100-240*	*0.687* *19.6*	*1.31* *1.32*	
SNACs	*Pb* *Cu* *Hg*	*101.4-1533.9* *198-1982* *61.8-768.75*	*1.5* *4.94* *1.3*	*0.386* *0.4* *0.29*	56
Au Microband	***Pb*** ***Cu*** ***Hg***	***3-100*** ***10-100*** ***1-75***	***1.3*** ***0.9*** ***0.8***	***5.27*** ***3.57*** ***2.45***	This Work

Electrochemical pH control

All the previous experiments were carried out with an interdigitated gold microband electrode of 2µm gap, and a blank solution, made of DI and NaCL, acidified by adding different volumes of HNO_3, (depending on the metal). For electrochemically controlled pH it would be necessary to generate H^+ ions by polarizing a protonator electrode. To further understand the diffusion of H^+ ions in solution, finite element analysis simulations were undertaken as described in the experimental section. The simulated change in pH of a solution following application of galvanostatic currents of 1 nA, 10 nA and 100 nA (for 0.1 s) is shown as profiles in Figure 3. As the galvanostatic currents increased, the flux of protons from the protonator increased, resulting in a lower pH simulated at the central working electrode. Protons were generated at each of the 14 protonator microbands. As these protons diffused radially outwards, diffusion zones overlapped to create an area of reduced pH over the adjacent sensing electrode. The model predicted an initial sharp decrease in pH, which then largely stabilizes. At an applied current of 100 nA, the pH at the central working electrode decreased from pH 7 to pH 3.27 after 100 ms, to pH 2.96 after 1 second and then to stable pH 2.78 after 10 seconds. A minimal decrease in pH was predicted after this as the generation of protons was matched by their diffusion (pH 2.62 after 200s). The simulations indicated that a galvanostatic current of 100 nA was required to achieve the optimum pH (pH 3.5) for the detection of mercury and lead.

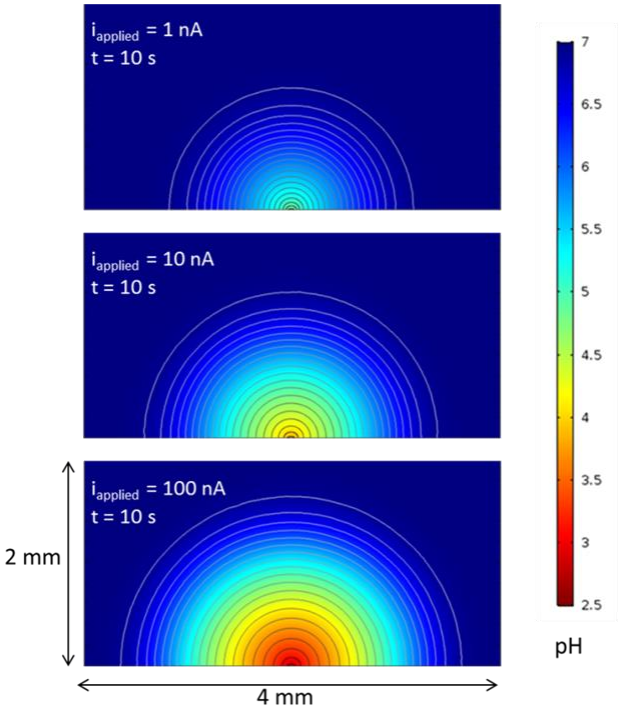

Figure 3 Simulated pH profile close to the electrode when (a) 1, (b) 10 and (c) 100 nA are applied on the protonator

To confirm this simulation model, CVs were carried out in DI water in the potential range from 0 to 1.2 V vs Ag/AgCl (scan rate 100mV/s) using the 'sensing electrode' as a working electrode while simultaneously applying a constant potential to the protonator electrode. The pH of the solution was measured in-situ using the potential of the AuO/Au reduction peak as a metric of pH. The AuO reduction peak potential in a solution of pH 6 (DI water and NaCl), was observed to be 0.41V (vs. Ag/AgCl) while, adjusting pH to 3.5 (using nitric acid), the peak position shifted to 0.72V (vs. Ag/AgCl). Consequently, if the local pH decrease when polarizing the protonator electrode, the peak voltage of the AuO reduction peak would be expected to move consistently. The effect of the applied potential on the protonator electrode, on CVs recorded with the sensing electrode is shown in Figure S5. When the applied potential to the protonator electrode is higher than 1.3V vs. Ag/AgCl the AuO/Au reduction peak potential maximum starts to move towards more anodic potentials and reaches 0.72 (V s Ag/AgCl) equivalent to pH 3.5, when the applied potential is set at 1.74V (See Figure S5). Moving from this result, SWASVs experiments with different concentrations of copper, mercury and lead separately in a solution containing only NaCl 10mM in DI (pH 6) were carried out by applying a constant potential of 1.74V to the protonator electrode. Figure 4a shows the SWASV of 50 ppb of mercury in three different pH conditions: i) solution at pH 7 (blue line), ii) solution at pH 7 with the protonator electrode polarized at +1.74V (red line) and iii) a solution chemically acidified to pH 3.5 (black line). From Figure 4a, it can be observed that the mercury (or other metals) deposition/stripping does not occur at pH 7.0 – blue line. However, by altering the pH locally, in the vicinity of the sensing electrode, by biasing the protonator with a constant voltage of 1.74 V, a Hg stripping peak is now observed at ~0.52V (Vs Ag/AgCl). To confirm this result arose from the adjustment of local pH by the protonator electrode, the bulk solution pH was chemically adjusted, to ~pH 3.5, (by adding of nitric acid dropwise) and the deposition/stripping experiment repeated.

A Hg stripping peak was again observed with a peak maximum occurring at ~0.55V (Vs Ag/AgCl). This peak had a similar intensity to the electrochemically pH adjusted peak, but was slightly shifted to a more anodic potential (due to slight differences in final pH arising from the acid addition method). Having shown that local pH control was sufficient to allow detection of mercury, work then focused on determining linearity and limits of detection for mercury, copper and lead. Figures 4 b, c, d show the effect of increasing concentration of Hg, Cu and Pb using a standard addition approach, applying + 1.74 V (vs Ag/AgCl) to the protonator electrode. For copper and mercury, a minimum detection concentration of 5 ppb was achieved for both metals. However, a decrease in the sensitivity of about 30% was observed for copper detection, compared to the acid modified pH. This is probably due to the pH: as the potential applied to the protonator, was only sufficient to decrease the pH to ~ 3.5, which is not the optimum pH for copper detection. In Figure S1a it is shown that the peak Cu stripping current at pH 3.5 is 28% lower than the peak current at pH 2. This strongly supports that the decrease in sensitivity arose from sub-optimal pH being applied during the deposition process.

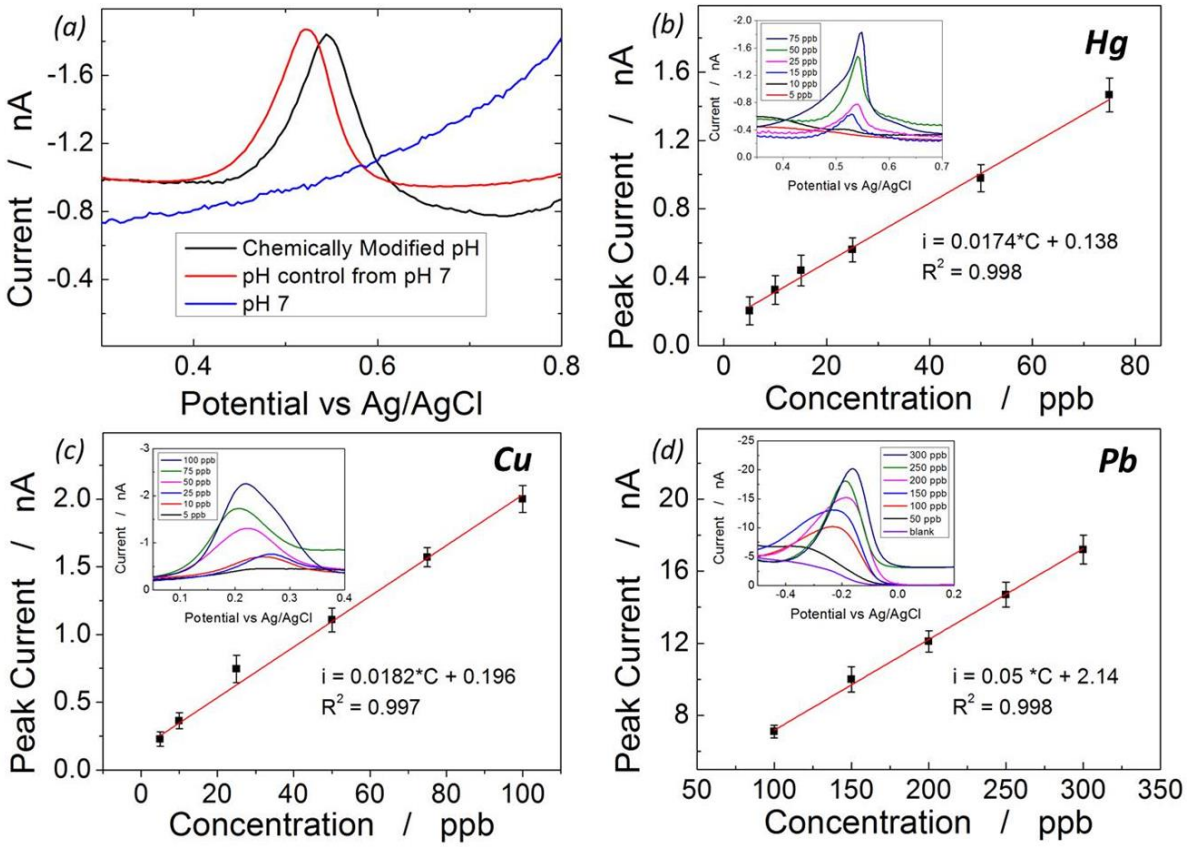

Figure 5 Effect of increasing concentration of (a) Cu (b) Pb and (c) Hg and corresponding calibration line (insets) using river water with chemically modified pH (3.5). (d) Effect of increasing concentration of copper and standard addition method (inset) using untreated river water with electrochemically pH control 3.5

Concerning lead, a decrease in LOD was found because of the overlap with the oxygen reduction peak overlapping with the lead stripping peak. This remains a challenge even if the solution were degassed due to the water splitting reaction, used to reduce the pH locally, producing molecular oxygen. This secondary effect poses a problem for lead detection with

pH control technique: the peak height of oxygen is more than twice, compared with the blank solution at pH3.5 (Figure S6). This enhancement significantly decreases the LOD for lead with the pH control. In order to see the lead peak in these condition the minimum concentration is 100 ppb (Fig 4d).

River Water Analysis and interference

In order to evaluate the possibility of using our sensors with complex water samples, three different river water samples were collected on different days and on different spots from the River Lee, Cork, Ireland. After the addition of 10 mM NaCl, the pH of samples 1 and 2 were chemically adjusted by adding 1 mM nitric acid while the pH of sample 3 was adjusted electrochemically. For calibration purposes, a standard addition method was again undertaken, and repeated in triplicate for each sample

River Water analysis with chemically modified pH

Following nitric acidification of samples 1 and 2, peaks for both mercury and lead (expected at 0.522 V and -0.17 V, respectively) were absent indicating that these metals were either not present, or present at values lower than our LOD, by contrast, a peak was observed at ~0.22V and was attributed to copper (see Figure S7).
After spiked addition of different concentrations of copper and lead to sample 1 and mercury to sample 2, they were detected by the sensor under development, confirming the ability to detect these metals together also in the river water (Figure 5 a,b,c). The results show that the proposed method for copper, mercury and lead determination in river water is efficient and applicable. Furthermore, it is important to highlight that for each sample, the predicted copper concentration with the standard addition method (34 ppb in case of Sample 1) is close to the concentration obtained using the calibration line in DI+NaCl+HNO_3 (43 ppb). This result suggests that the matrix of the river water has slight influence on the performance of the sensor.

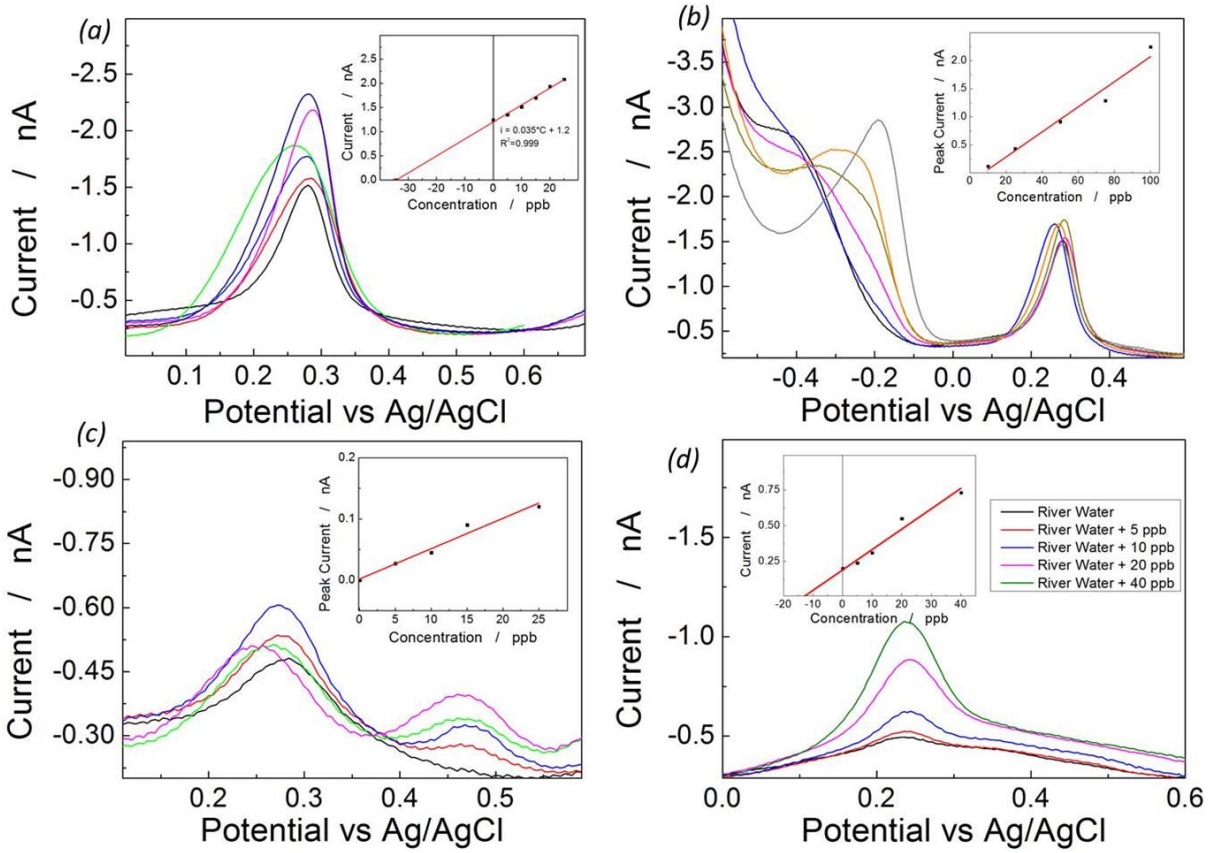

Figure 6 Effect of increasing concentration of (a) Cu (b) Pb and (c) Hg and corresponding calibration line (insets) using river water with chemically modified pH (3.5). (d) Effect of increasing concentration of copper and standard addition method (inset) using untreated river water with electrochemically pH control 3.5

Reagent free river Water analysis

As previously mentioned, river water sample 3 was used to detect copper using the electrochemical pH control procedure. The results are shown in Figure 5d. Also in this case, the sensing electrode detected copper, finding a content of 13 ppb using the standard addition method (fig5d). Here again, the concentration predicted by the standard addiction method is close to the one predicted by the calibration line of Figure 4c (8.2 ppb). This is an important result because it validates the method. Indeed, the river water sample was not treated at all and it was tested as collected.

Interference study

From Fig. 5, it is evident that a sensor electrode can detect the metals also when they are present together. Indeed, the electrode is able to detect increasing concentration of Hg and Pb also in presence of Cu (Figure 5 b and c). However, the presence of other metals present in the sample affects the detection when compared to individual metals. For example, the copper peak is enhanced (compared to the peak when only copper is present) when mercury and lead are present while the mercury peak is slightly decreased when copper and lead are present. El Tall et al. found a similar result when tried to detect lead in the presence of copper, and attributed this effect to the deposition of a Cu/Pb alloy or competition for the binding sites [47-48].
This effect is probably due to the formation of an alloy between these metals [49]. In the mentioned work, Agra Gutierrez et al. showed that there is a big interference on the detection

of copper when lead is present but they found a different behavior, with a decreasing of copper peak height when lead concentration increases. A similar issue has been found by Sayen et al. when tried to detect copper in the presence of mercury [50]. This behavior was also found by other authors [51-52]. In any case, to ad-dress this effect, a good approach would be to calculate different calibration lines, not only in presence of the tar-get metal but also with the 'interference' one.

Conclusion

A multi heavy metals sensing electrode has been success-fully fabricated depositing an array of interdigitated gold microband on SiO2 substrate. In particular, the gold microbands electrode was obtained through photolithography. The electrochemical measurements were carried out in DI water adding NaCl to increase the conductibility and nitric acid to modify the pH. The LOD for all the tested metals was lower than the limit established by EPA, evidencing that this technique is applicable and powerful. When copper, lead and mercury were simultaneously pre-sent in the solution some interference is seen, especially for detecting lead. However, the interference is negligible and the metal quantification is still possible. Furthermore, an innovative method to control the pH close to the electrode was found. H+ generation through water electrolysis under constant potential of the protonator electrode al-lowed local pH control at the surface of the sensing electrode. The metal stripping response at a controlled was very similar to that when the pH was externally modified. With this technique, the sensor was able to work at a neutral pH, avoiding any sample pretreatment and metals digestion. The electrode is also able to detect these metals in a real matrix water such as river water, from Lee River in Cork, Ireland. This work demonstrates how electrochemical sensors can solve the problems of analytical techniques, like costs, portability and simplicity, opening new opportunities in the field of sensors for environmental analysis.

Acknowledgements

The authors would like to acknowledge funding from the Irish EPA UisceSense Project (Code: 2015-W-MS-21). This work has been supported in part by a research grant for the VistaMilk Center Science Foundation Ireland (SFI) and Department of Agriculture Food and the Marine (DAFM) under Grant Number 16/RC//3835

References

1 https://eur-lex.europa.eu/legal-content/EN/TXT/?uri=celex:32000L0060 (Accessed Jul, 2020)
2 https://ec.europa.eu/info/sites/info/files/com_report_wfd_fd_2019_en_1.pdf (Accessed Jul, 2020)
3https://www.un.org/sustainabledevelopment/sustainable-development-goals/ (accessed Apr 16, 2019)
4 A. Ivankovic, A. Dronjic, A.M. Bevanda, S. Talic, Int. Journ. Sust. Green En., 2017, 6, 39-48 ,
5 C.M.A. Brett, Pure and App. Chem., 2007, 79, 1969-1980
6 P. Yáñez-Sedeño, S. Campuzano, J.M. Pingarrón, Current Opinion Green Sust. Chem., 2019, 19, 1-7
7 EPA method 3050B, Acid digestion of sediments, sludges and soils
8 S. J. Cobbina, A. B. Duwiejuah, R. Quansah, S. Obiri , N. Bakobie, Int J. Environ. Res Public Health. 2015; 12, 10620–10634.
9 N. Ratner, D. Mandler, Anal. Chem., 2015, 5148-5155
10 http://apps.who.int/food-additives-contaminants-jecfa- database/search.aspx?fcc=2 (accessed Apr 15, 2019)
11 Apple P., L. Na-Oy, J. Env. Prot., 2014, 5, 493-499
12 Järup L., Br. Med. Bull., 2003, 68, 167-182.
13 L.M. Gaetke, C.K. Chow, Toxycology, 2003, 189, 147-163
14 National Primary Drinking Water Regulation, US-EPA

https://www.epa.gov/ground-water-and-drinking-water/national-primary-drinking-water-regulations
15 Water Framework Directive (consolidated): Directive 2013/39/EU of the European parliament and of the council
16 A.K. Tareen, I.N. Sultan, P. Parakulsuksatid, M. Shafi, A. Khan, M.W. Khan, S. Hussain, Int.J.Curr.Microbiol.App.Sci, 2014, 3, 299-308
17 V.L. Dressler, D. Pozebon, A.J. Curtius, Spectrochim. Acta B Atomic Spectr., 1998, 53, 1527-1539
18 C. Sunseri, C. Cocchiara, G. Ganci, A. Moncada, R.L. Oliveri, B. Patella, S. Piazza, R. Inguanta, Chem. Eng. Trans., 2016, 47, 43-48
19 B. Patella, R. Inguanta, S. Piazza, C. Sunseri, Sens.Act. B, 2017, 245, 44-54
20 B. Patella, C. Sunseri, R. Inguanta, J. Nanoscie. Nanotech., 2018, 18, 1-12;
21 R. Ramachandran, S. Chen, G. Kumar, P. Gajendran, N. Devi,, Int. J. Electrochem. Sci., 2015, 10, 8607 – 8629
22 S. Barry, K. Dawson, E. Correa, R. Goodacre, A. O'Riordan. Faraday discussions. 2013;164:283-93.
23 T. L. Read, E. Bitziou, B. Maxim, J. Macpherson, V. Macpherson , Anal. Chem., 2014, 86, 367–371
24 A.J. Wahl, S. Barry, K. Dawson, J. MacHale, A.J. Quinn, A O'Riordan, J. Electrochem. Soc., 2014, 161, B3055-B3060
25 A. Shrivastava, V.B. Gupta, Chron. Young Scientiest, 2011, 2, 21-25
26 R. A. Robinson, R. H. Stokes, Electrolyte Solutions; Butterworth. 1959
27 K. Dawson, M. Baudequin, A. O'Riordan, Analyst, 2011, 136, 4507-4513
28 A.J. Wahl, I.P. Seymour, M Moore, P Lovera, A. O'Riordan J.F. Rohan. Electrochimica Acta. 2018 Jul 1;277:235-43.
29. B. Patella, R. Inguanta, S. Piazza, C. Sunseri, Chem. Eng. Trans., 2016, 47, 19-24
30 M. Eduardo, J. J. Pedrotti, L. Angnes, Electroanal., 2003, 15, 1871-1877
31 C. Zhang, Y. Zhou, L. Tang, G. Zeng, J. Zhang, B. Peng, X. Xie, C. Lai, B. Long, J. Zhu, Nanomat., 2016, 6, 1-11
32 X. Xuan, M.D.F. Hossain, J.Y. Park, Scient. Rep., 2016, 6, 1-8
33 S. A. Trammel, D. Zabetakis, M. Moore, J. Verbarg, D. A. Stenger, Plos One, 2014, 9, 1-12
34 D. Zhang, Y. Fang, Z. Miao, M. Ma, Q. Chen, Journ. App. Electrochem., 2014, 44, 419–425
35 O. Berkh, H. Ragones, D. Schreiber, L. Burstein, Y. Shachman-Diamand, Journ. App. Electrochem, 2012, 42, 491–499
36 G. Martinez-Paredes, M. B. Gonzalez-Garcia, A. Costa-Garcia, Electrochim. Acta, 2009, 54, 4801-4808
37 E. Kirowa-Eisner, Y. Bonfil, D. Tzur, E. Gileadi, Journ. Electroanal. Chem,, 2003, 552, 171-183
38 A. Hamelin, J. Lipkowski, J.Electroanal. Chem, 1984, 171, 317
39 M.F. Noh, F. Tothill, Anal. Bioanal. Chem., 2006, 386, 2095-2106
40 A.R. Thiruppathi, B. Sidhureddy, W. Keeler, A. Chen, Electrochem. Comm., 2017, 76, 42-46
41 P.J. Mafa, A.O. Idris, N. Mabuba, O.A. Arotiba, Talanta, 2016, 153, 99-106
42. S. Hao, J. Li, Y. Li, Y. Zhang, G. Hu, Anal. Meth., 2016, 8, 4919-4925
43 L. Yu, P. Zhang, H. Dai, L. Chen, H. Ma, M. Lin, D. Shen, RSC Adv., 2017, 7, 39611-39616
44 X. Li, H. Wen, Q. Fu, D. Peng, J. Yu, Q. Zhang, X. Huang, App. Surf. Sci. 2016, 363, 7-12
45 S. Deshmukh, G. Kandasamy, R.K. Upadhyay, G. Bhattacharya, D. Banerjee, D. Maity, M.A. Deshusses, S. S. Roy, Journ., Electroanal. Chem., 2017, 788, 91-98
46 Z. Koudelkova, T. Syrovy, P. Ambrozova, Z. Moravec, L. Kubac, D. Hynek, L. Richtera, V. Adam, Sensors (Basel), 2017, 17, 1832
47 O. Diaz-Moralez, F. Calle-Vallejo, C. De Munck, M.T.M. Koper, Chem. Sci., 2013, 4, 2334-2343
48 S. Goubert-Renaudin, M. Moreau, C. Despas, M. Meyer, F. Denant, B Lebeau, A. WAlcarius, Electroanal., 2009, 21, 1731-1742
49 C. Agra-Gutierrez, J. L. Hardcastle, J. C. Ball, R. G. Compton, Analyst, 1999, 124, 1053-1057
50 S. Sayen, C. Gerardin, L. Rodehuser, A. Walcarius, Electroanal., 2003, 15, 442-430
51 C. Babyak, R. B. Smart, Electroanal., 2004, 16, 175-182
52 D. Dragoe, N. Spataru, R. Kawasaki, A. Manivannan, T. Spataru, D. A. Tryk, A. Fujishima, Electrochim. Acta, 2006, 51, 2437-2441
53 H. Xing, J. Xu, X. Zhu, X. Duan, L. Lu, Y. Zuo, Y. Zhang, W. Wang, Journ. Electroanal. Chem, 2016, 782, 250-255
54 L.L. Shen, G.R. Zhang, W. Li, M. Biesalski, B.J.M. Etzold, ACS Omega, 2017, 5, 4593-4603
55 Y.F. Sun, L.J., Zhao, T.J. Jiang, S.S. Li, M. Yang, X.J. Huang, Journ. Electroanal. Chem., 2016, 760, 143-150
56 R. Madhu, K.V. Sankar, S.M. Chen, R.K. Selvan, RSC Adv., 2014, 4, 1225-1233